AIAA 2017-4973
AIAA Propulsion and Energy Forum
10-12 July 2017, Atlanta, GA
53rd AIAA/SAE/ASEE Joint Propulsion Conference

Passive High-speed Imaging of Ion Acoustic Turbulence in a Hollow Cathode

Marcel P. Georgin*, Matthew P. Byrne †, Nikolas E. Ciaston ‡, Benjamin A. Jorns§ and Alec D. Gallimore¶

University of Michigan, Ann Arbor, MI, 48109, USA

A passive, non-invasive plasma diagnostic is developed and validated to estimate the dispersion of electric propulsion plasmas. This new technique uses a Silicon photomultiplier (SiPM) to measure fluctuations in light intensity to estimate the dispersion of the plasma. Experimental validation of the technique was conducted on a hollow cathode. Ion acoustic waves, which are responsible for the anomalous resistivity of the cathode plume, were measured using both ion saturation probes and the SiPM technique. The results from the SiPM were compared to measurements from ion saturation probes. While the raw data and power spectra acquired with the SiPM were different, the estimated dispersion and phase velocity are within uncertainty of each other and within uncertainty of similar measurements found in the literature.

Nomenclature

ΔV	=	Overvoltage
Δx	=	Probe or pixel spacing
ϵ	=	Cutoff energy of the optical emission cross section
ω	=	Frequency
ϕ	=	Plasma potential fluctuation
σ_0	=	Total Xe ion optical emission cross section
$\theta(\epsilon)$	=	Heaviside step function.
$\tilde{I}$	=	Fluctuation in the light emission intensity
$\tilde{n}$	=	Fluctuation in the plasma density
C	=	Microcell capacitance
c_s	=	Ion sound speed
$D(k,\omega)$	=	Dispersion function
E	=	Electron energy
G	=	Gain
I	=	Light emission intensity
I_0	=	Steady state light emission intensity
k	=	Wavevector
M	=	Number of trials
m_i	=	Ion mass
n	=	Plasma density
n_0	=	Steady state plasma density
n_n	=	Neutral density
$P(\omega)$	=	Power spectrum

*Ph.D. Candidate, Applied Physics, AIAA Student Member.
†Ph.D. Pre-Candidate, Applied Physics, AIAA Student Member.
‡Master's Student, Aerospace Engineering, AIAA Student Member.
§Assistant Professor, Aerospace Engineering, AIAA Senior Member.
¶Robert J. Vlasic Dean of Engineering, the Richard F. and Eleanor A. Towner Professor of Engineering, and an Arthur F. Thurnau Professor of Aerospace Engineering, and AIAA Fellow.

q	=	Electron charge
T_e	=	Electron temperature
u_i	=	Ion drift velocity
v_{ph}	=	Phase velocity
IAT	=	Ion acoustic turbulence
SiPM	=	Silicon photomultiplier

I. Introduction

The Hall thruster is an electric propulsion technology that uses crossed electric and magnetic fields to accelerate ions and efficiently produce thrust (70% total efficiency). In the commercial sector, Hall thrusters are primarily used for orbit maintenance, but can also be used for orbit raising because of their relatively high thrust (400 mN at 6 kW). For government space agencies, electric propulsion has been used for deep-space exploration [1] and scientific missions [2,3]. In the future, electric propulsion will play a role in manned missions to Mars. [4] In particular, higher power Hall thrusters are being developed at NASA's Jet Propulsion Laboratory and Glenn Research Center to enable deep space robotic missions [5]. These NASA centers have partnered with Aerojet Rocketdyne and the University of Michigan to develop a 100 kW Hall thruster in support of manned Mars missions.

For deep space exploration, Hall thrusters would require continuous use for about 50,000 hours (about 6 years). Flight qualification of a Hall thruster for this kind of mission is prohibitively time consuming and expensive. The solution to this problem is to develop numerical plasma physics models that predict Hall thruster performance and lifetime. To date, Hall thruster codes rely on empirical laws to match the performance of real thrusters. Notably, these numerical models use an anomalous collision frequency to model electron transport in the cathode plume and in the near field region of the Hall thruster.

The presence of ion acoustic turbulence (IAT) in the hollow cathode plume of Hall thrusters was initially integrated in numerical codes to resolve the inconsistencies in the anomalous electron resistivity in the cathode plume. [6] Theoretical work has shown that IAT can be present in the cathode plume and can result in an effective collision frequency. [7] Since its original use in numerical models, experimental investigations into the presence of ion acoustic turbulence in the cathode plume have shown that both the anomalous resistivity and the presence of high energy ions in the cathode plume are a result of this electrostatic instability. [8,9] IAT redistributes the electron kinetic energy to electron and ion thermal energy. The wave onsets when the electron drift velocity is large enough to overcome damping caused by ion-neutral collisions and Landau damping. Measurements in standalone hollow cathodes have been made using ion saturation probes to show that IAT is present in the hollow cathode plume [8]; however, the onset of the anomalous resistivity in the hollow cathode remains poorly understood.

While measurements of IAT have been made in hollow cathodes, no such measurements have been made in the channel of a Hall thruster. The measurements of IAT in hollow cathodes used an array of ion saturation probes to estimate the dispersion of the plasma and showed that the wave was present [8]. This measurement technique, however, is slow and the probes would not survive in the thruster channel. In addition, the presence of probes near the thruster channel has been shown to perturb the operation of the thruster. [10,11] As a result, there is an apparent need to develop a non-invasive plasma diagnostic to measure IAT in the channel of a Hall thruster to see if it is responsible for the anomalous resistivity in the near field plume.

IAT manifests itself at a frequency range of 1 MHz to about 5 MHz, therefore any new diagnostic that can be used to estimate the dispersion of ion acoustic instabilities must must have sufficient bandwidth to cover that frequency range. In addition, the diagnostic needs to be non-invasive as to not perturb the operation of the thruster. To satisfy these requirements, the technique developed in this paper uses a silicon photomultiplier (SiPM) array to detect fluctuations in emitted light from the plasma. An SiPM is a semiconductor chip that can be used in a similar way to a traditional photomultiplier to detect light. These SiPMs have a large gain (10^6) and can be purchased in an array of up to 8×8. The spatial distribution of the SiPM array allows several spatial points to be measured simultaneously at high speed, (4 MHz). By imaging the plasma onto two SiPM pixels, the dispersion of the plasma can be estimated like the ion saturation probe technique. [8]

II. Theory

A. Ion Saturation Probes

Jorns et al. experimentally confirmed the presence of ion acoustic turbulence using an array of ion saturation probes.[8] Under the assumption of an unmagnetized, collisionless plasma, the fluctuation of the plasma potential for an electrostatic mode, such as ion acoustic waves, can be related to plasma density fluctuations by:

$$\phi \simeq \frac{T_e}{q}\frac{\tilde{n}}{n_0} \tag{1}$$

Where T_e is the electron temperature, $\tilde{n}$ is the fluctuation in the plasma density and n_0 is the equilibrium plasma density. Since the ion saturation current is proportional to the plasma density, fluctuations in the ion saturation current can be used to estimate the fluctuation in the plasma potential, assuming the oscillation in the electron temperature is small:

$$\phi \simeq \frac{T_e}{q}\frac{\tilde{i}_{sat}}{\bar{i}_{sat}} \tag{2}$$

Where the $\tilde{i}_{sat}$ is the fluctuation in the ion saturation current and $\bar{i}_{sat}$ is the steady state ion saturation current. By computing the correlation between the signals from two spatially separated saturation probes, the dispersion, $D(k,\omega)$, of a wave can be estimated.[12] The presence of electrostatic probes, however, has been known to perturb the properties of the plasma and could be influencing the measurement of the instability. This motivates the development of noninvasive techniques to measure plasma waves in locations that are not accessible by probes.

B. Silicon Photomultiplier

As a proof of concept, an SiPM array was used to passively and noninvasively measure the ion acoustic instability present in high current hollow cathode plumes[7,8]. The goal is to measure high speed fluctuations in the light intensity to estimate wave properties such as the dispersion and phase velocity. The intensity of the light, I produced by the cathode should be:

$$I = n_n n \int_0^\infty \sqrt{\frac{2qE}{m_e}}\sigma_{emis}(E) f(E) dE \tag{3}$$

where E is the electron energy in eV and σ_{emis} is the optical emission cross-section. If we assume that the plasma is Maxwellian, then the expression simplifies to:

$$I \simeq n_n n T_e^{-3/2} \int_0^\infty \sigma_{emis}(E) e^{-\frac{E}{T_e}} E dE \tag{4}$$

The optical emission cross-section for xenon vanishes below a threshold energy ϵ, which is about 10 eV[13]. Since the electron temperature in the cathode plume is about 3 eV for most cathodes, only the high energy tail of the distribution will generate optical excitation. Computing the integral after approximating the $\sigma_{emis} \simeq \sigma_0 \theta(\epsilon)$, we find:

$$I \simeq n_n n \sigma_0 \sqrt{T_e} e^{-\frac{\epsilon}{T_e}} \frac{T_e + \epsilon}{T_e} \tag{5}$$

$$\simeq n_n n \sigma_0 \sqrt{T_e} e^{-\frac{\epsilon}{T_e}} \left(1 + \frac{\epsilon}{T_e}\right) \tag{6}$$

If we assume that the electron temperature is near the cut-off energy, then we can series expand the exponential as:

$$I \simeq n_n n \sigma_0 \sqrt{T_e} \frac{1}{e}\frac{T_e}{\epsilon} \left(1 + \frac{\epsilon}{T_e}\right) \tag{7}$$

$$\simeq n_n n \sigma_0 \sqrt{T_e} \left(1 + \frac{T_e}{\epsilon}\right) \tag{8}$$

Assuming that the neutral density is not varying at high frequency and that the electron temperature is not fluctuating, then the relative fluctuation in optical emission is proportional to the relative fluctuation in density:

$$\frac{\tilde{I}}{I_0} \simeq \frac{\tilde{n}}{n_0} \tag{9}$$

where I_0 and n_0 are the steady state light intensity and plasma density and $\tilde{I}$ and $\tilde{n}$ are the fluctuations in light intensity and plasma density. Eqn. 9 allows us to exchange the ion saturation current measurement from the probes with the light intensity fluctuation measurement from the SiPM detector and as the proxy for density fluctuations.

$$\phi \simeq \frac{T_e}{q}\frac{\tilde{I}}{I_0} \tag{10}$$

By similarly computing the correlation between the two pixels, a map of the dispersion relation can be generated using the technique developed by Beall[12]. This analysis makes similar assumptions to those for the ion saturation probes; however, the caveat is that the measured intensity is both line integrated through the plasma and spatially averaged over the image of the plasma in the pixel.

This new experimental technique is validated against measurements from the ion saturation probe method and is used to estimate wave properties in a 20 A hollow cathode designed at the Plasmadynamics and Electric Propulsion Laboratory (PEPL) for the H6 Hall thruster. This investigation examines both the validity of the new diagnostic and searches for ion acoustic waves in hollow cathodes at lower currents 45-55 A compared to the measurements made by Jorns et al (100 A)[8].

C. Analysis Technique

The measured traces from the probes and the SiPM are analyzed using a dispersion estimation technique similar to that developed by Beall[12]. The technique is predicated on the eikonal approximation[8]:

$$\phi = \sum_{\omega} \phi(\omega) e^{i(k(\omega)x - \omega t)} \tag{11}$$

Which assumes that for frequency ω, there exists one wavevector $k(\omega)$. By capturing a signal from two probes (or SiPM pixels) with a fixed spacing, $x_1 - x_2 = \Delta x$, the signals can be decomposed using eqn. 11 as:

$$\phi_1 = \sum_{\omega} \phi_1(\omega) e^{i(k(\omega)x_1 - \omega t)} \tag{12}$$

$$\phi_2 = \sum_{\omega} \phi_2(\omega) e^{i(k(\omega)x_2 - \omega t)} \tag{13}$$

By taking the Fourier transform of these signals, the wavevector can be found by:

$$k(\omega) = \frac{1}{\Delta x} \tan^{-1}\left(\frac{\mathrm{Im}(F(\phi_2)F(\phi_1)^*)}{\mathrm{Re}(F(\phi_2)F(\phi_1)^*)}\right) \tag{14}$$

This technique essentially estimates the wavevector by finding the phase between two signals at a known probe separation. In a plasma, however, there can be multiple modes present. Therefore a single estimation of the wavenumber for a particular frequency may be errant. To achieve a more realistic estimation of the dispersion in the plasma, we will employ the statistical analysis first proposed by Beall to determine a two dimensional power spectrum in ω and k space. The power spectrum in ω space, $P(\omega)$, is found by computing the Fourier transform of the time trace. To produce a power spectrum in k space, $P(k)$, $k(\omega)$ must be estimated M times and binned. To produce the two dimensional power spectrum, $S(\omega, k)$, $P(k)$ must be weighted by the power spectrum $P(\omega)$. Because $k(\omega)$ is estimated from two traces, $P(\omega)$ should the average power spectrum of the traces. Mathematically the binning is written as:

$$S(k,\omega) = \frac{1}{M}\sum_{j=1}^{M} I_{0,\Delta k}(k - k^j(\omega))\frac{1}{2}(P_1^j(\omega) + P_2^j(\omega)) \tag{15}$$

Where j indicates a run number and the function:

$$I_{0,\Delta k}(k - k^j(\omega)) = \begin{cases} 1 & |k - k^j(\omega)| < \Delta k \\ 0 & |k - k^j(\omega)| > \Delta k \end{cases} \tag{16}$$

Where Δk is the bin width. This algorithm essentially generates a $P(k)$ weighted by $P(\omega)$. Using this statistical description to estimate the dispersion relaxes the original assumption that there exists a single $k(\omega)$ and allows us to visualize the dominant dispersion content of the plasma.

Based on this analysis technique[8], the maximum k that can be observed by the probes (or SiPM) is related to the distance between the two probes:

$$k_{max} = \frac{\pi}{\Delta x} \tag{17}$$

where Δx is the spacing between the probes. The maximum cutoff frequency that can be observed by the system is limited by the size of the probe (or pixel). In this work, we are searching for acoustic waves, therefore:

$$f_{cutoff} = \frac{v_{ph}}{2\delta x} \tag{18}$$

where v_{ph} is the phase velocity and δx is the width of the probe.

D. Ion Acoustic Turbulence

In this work, the theory developed by Jorns will be used analyze the estimated dispersion.[7,8] For an ion acoustic wave, the real component of the frequency is given by:

$$\omega_r = (c_s + u_i)\, k \tag{19}$$

where c_s and u_i are the ion sound speed and the ion drift velocity. The ion sound speed is given by:

$$c_s = \sqrt{\frac{2qT_e}{m_i}} \tag{20}$$

Previous measurements in hollow cathodes suggest that the phase velocity, ω/k of the wave should be approximately 6000 m/s.[8]

III. Experimental Methods

A. Hollow Cathode

The hollow cathode used for this experiment is the LaB_6 hollow cathode designed at PEPL for the H6 Hall thruster. The plasma discharge connects to a water-cooled tungsten anode 3.8 cm away that was provided by the electric propulsion group at NASAs Glenn Research Center. The cathodes nominal operating current is 20 A, however in this work the cathode was operated between 45 and 55 A.

B. Test Facility

The H6 cathode was tested in the cathode test facility at PEPL. The facility is 40 cm in diameter, 1 m long and uses a cryogenic pump with a pumping speed of 1500 L/s on Xe to achieve a base pressure of about 1×10^{-6} Torr-N_2. The typical operating pressures during cathode testing was 2×10^{-4} Torr-Xe.

C. Ion Saturation Probe Array

The saturation probe array is shown in Fig. 1. Probe 1 is nearest the anode and probe 2 is 2 mm upstream. These probes were used in this experiment to estimate the dispersion of the plasma in the axial direction. The tungsten electrode is 0.5 mm in diameter and protrudes 2 mm from the ceramic. The probes were placed at 2 cm from the cathode. Based on this probe configuration, Eqn. 18, and an estimated 6000 m/s phase velocity, the cutoff frequency for the probe setup is about 6 MHz.

An electrical schematic is shown in Fig. 2. The bias voltage to the probes was -36 V using batteries in series and the saturation current measurements were made using a commercially available oscilloscope across a 100 Ω resistor.

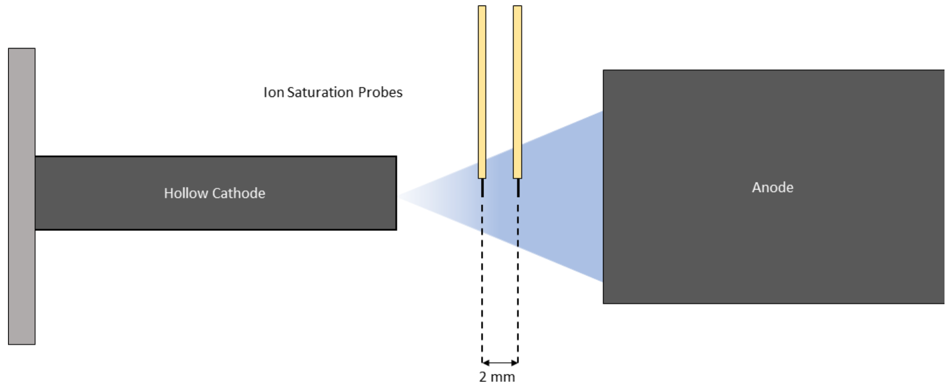

Figure 1: Ion saturation probe setup. The probes are spaced 2 mm apart and 2 cm from the cathode.

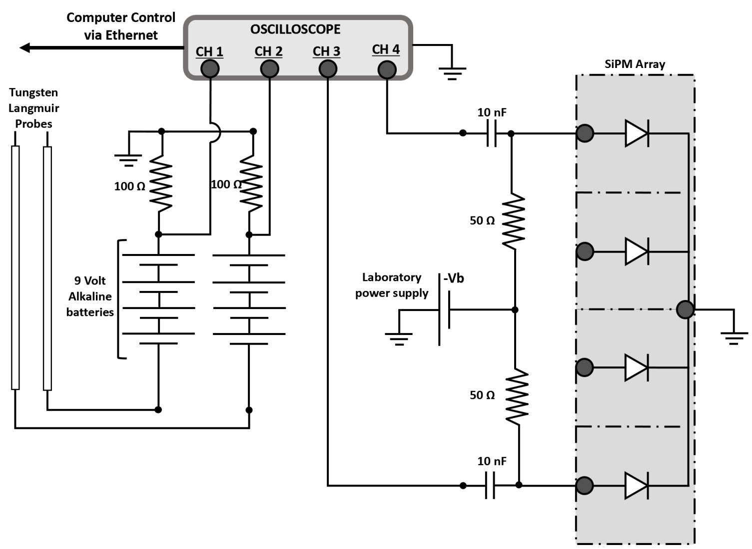

Figure 2: Circuit diagram of the experimental setup showing both the probes and SiPM.

D. Silicon Photomultiplier Array

The SensL inc. ArrayJ-30035-16P-PCB SiPM array, used in this study, is a 4×4 array of 16 J-series SiPMs, which are 3×3 mm^2 pixels. Each SiPM in the array is the functional equivalent to a photomultiplier tube (PMT), capable of achieving a gain greater than 10^6. The gain is controlled by the overvoltage, the amount of reverse voltage applied above the diode breakdown voltage. As shown in the eqn. 21, the gain is proportional to the overvoltage, with overvoltages of 2.5 to 5 V leading to typical gains of between 2.8×10^6 - 5.3×10^6

$$G = \frac{C \cdot \Delta V}{q} \tag{21}$$

where G is the gain, ΔV is the overvoltage, C is the microcell capacitance, and q is the electron charge.

The J-series SiPM has a large spectral range of 200 to 900 nm with peak photon detection efficiency at 420 nm. It also has a large frequency response, with a cutoff frequency of 4.3 MHz in standard output mode. As shown in Fig. 3, the SiPM detector was placed outside of the CTF and viewed the cathode through an acrylic window. The light was focused onto the SiPM array using a achromatic doublet. The SiPM cells were biased with a laboratory power supply and the output current was measured through a decoupling capacitor, which supplies AC current to the SiPM. This current is measured by an AC coupled oscilloscope.

With this experimental setup, each pixel collects approximately a 1×1 mm space in the plume of the cathode, or a magnification of 3. The two pixels used for the dispersion analysis were 9 mm apart from their

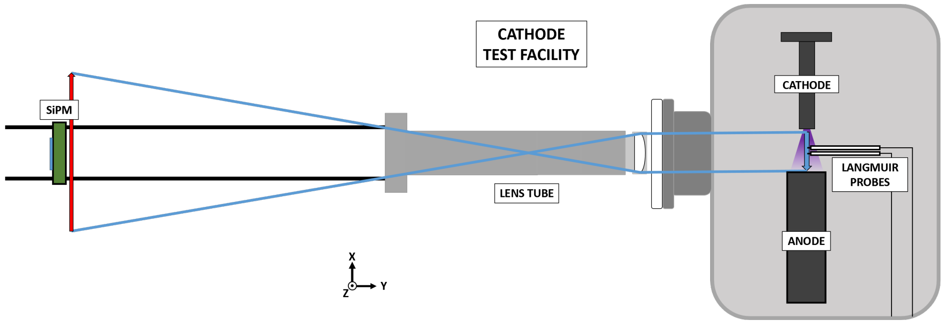

Figure 3: Silicon photomultiplier setup. The cathode plume is imaged onto the SiPM by an achromatic lens.

centers making the collected light 3 mm apart in the plume. Based on this configuration and Eqn. 18 and an estimated phase velocity of 6000 m/s, the cutoff frequency is expected to be about 3 MHz.

E. Calibration of the SiPM Circuit

The published documentation on the frequency response of the J-series SiPMs claims a cutoff frequency of 4.3 MHz for the standard output. The documentation also shows that the SiPM has different saturation intensities for each bias voltage, corresponding to the maximum current capable of being generated by the diode, and shows that response to light intensity should be linear up to 8 mA. Since this experiment involves measuring around 4 MHz over a wide range of intensities, we needed to verify that this device would work for our investigation.

To test the frequency response, an LED was pulsed with a GwINSTEK AFG-2225 arbitrary function generator with a 2.25 V sine wave and a 2.25 V DC offset, at frequencies varying from 1 to 5 MHz in 1 MHz increments. The light was then measured with the SiPM and a frequency analysis was preformed. The FFT of the resulting waveforms was plotted on a semi-log scale, as seen in Fig. 4b. This figure shows that the SiPM was capable of clearly measuring the driving frequency of the LED with less than a 1% error, and with peak intensities at least 3 orders of magnitude above the noise. The harmonics in the signal are likely due to asymmetric distortion of the LED signal. This distortion is a result of the non-linear dependence of the LED output at low input voltages.

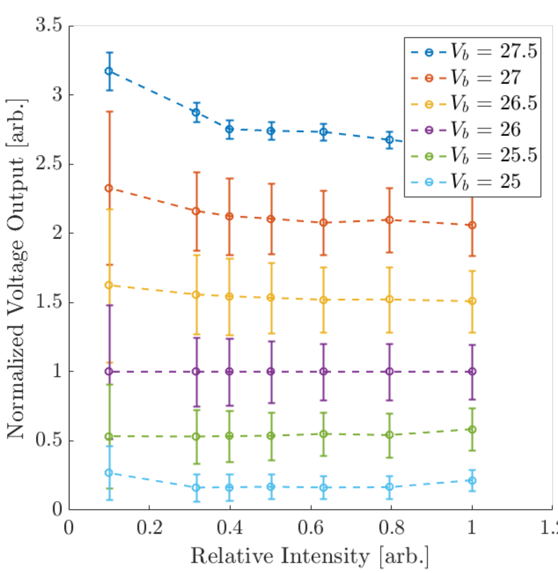

(a) Intensity calibration curves at different bias voltages. These curves are normalized by the intensity curve at $V_b = 26$ V.

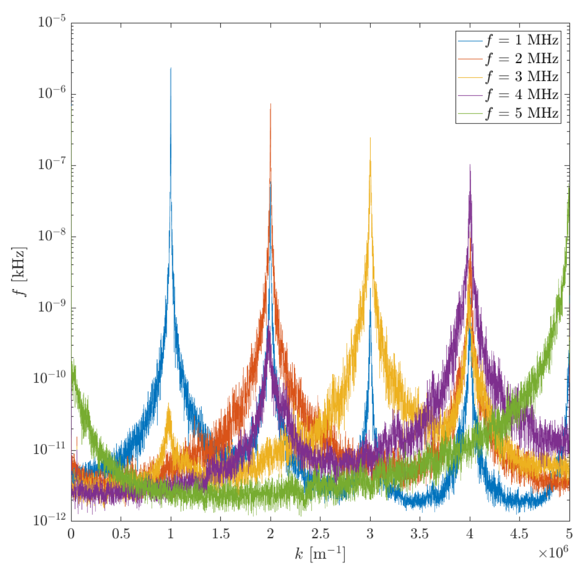

(b) Frequency calibration curves at LED driving frequencies between 1 and 5 MHz.

To test for intensity saturation, the LED was driven at 1 MHz and then blocked by successively stronger neutral density filters, ranging from 0 (no filter) to 1 OD in 0.1 OD increments. Beginning with the highest intensity light the SiPM was biased to 27.5 V with an average current of 8 mA, ensuring that the all of the subsequent measurements would fall within the documented linear region. Each intensity was measured at different bias voltages, ranging from 25.0 to 27.5 in 0.5 V increments. The results of these measurements are shown in Fig. 4a. In this figure we observe a linear response to intensity and bias voltage, indicating that indeed the SiPM is linear up to 27 V.

IV. Results & Discussion

The figures below show the results for the 55 A, 20 V, 5 sccm test condition. Raw measurements are shown in Fig. 5. Fig 5a shows the response from the probes. Qualitatively, the two probes have similar traces separated by a phase offset, as expected for a traveling wave. Fig 5b shows the response from the two SiPM pixels. In these traces a 50-kHz oscillation appears. The higher frequency oscillations do not show a clear phase relationship between the two pixels. From the raw traces, there are already some apparent differences in the response to plasma oscillations.

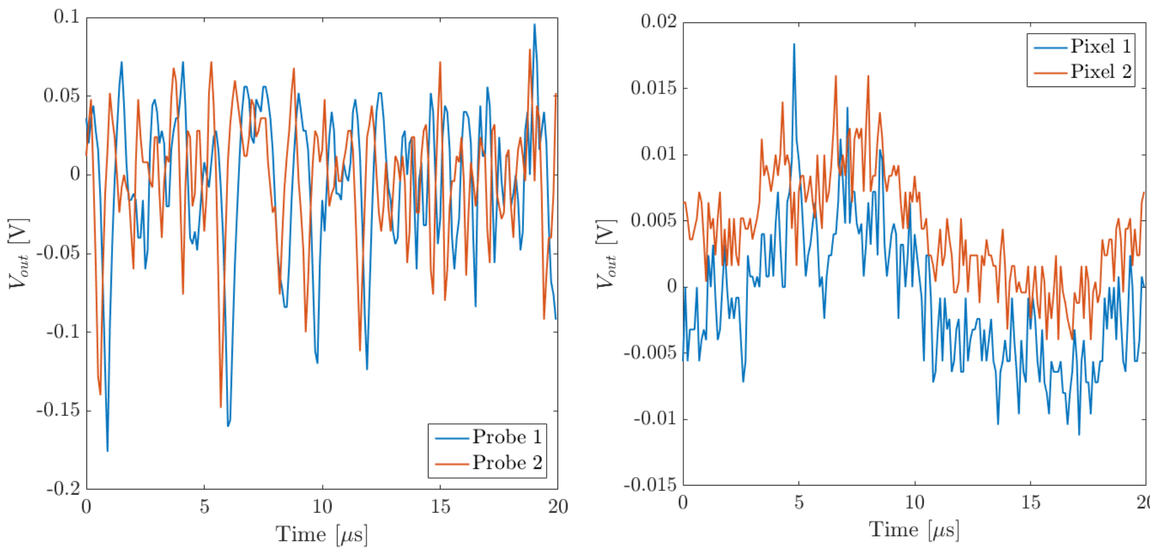

(a) Raw voltages measured by the probes.

(b) Raw voltages measured by the SiPM.

Figure 5: Comparison of the raw probe and SiPM signal over the first 20 μs during cathode operation at 55 A and 5 sccm.

To analyze these discrepancies further, the signals were Fourier transformed to explicitly examine the differences in the frequency content of the probes and the SiPM. The Fourier power spectrum is shown in Fig. 6. The major differences between these two traces is the dominance of the 50-kHz mode in the SiPM signal and the dominance of the broad, high-frequency (1 MHz) oscillation in the probe signal. This broad, high frequency content in the Fourier transform is associated with the presence of ion acoustic turbulence.[8] In the SiPM spectrum there exists a small concentration of power around 1 MHz which may be a result of ion acoustic wave detection.

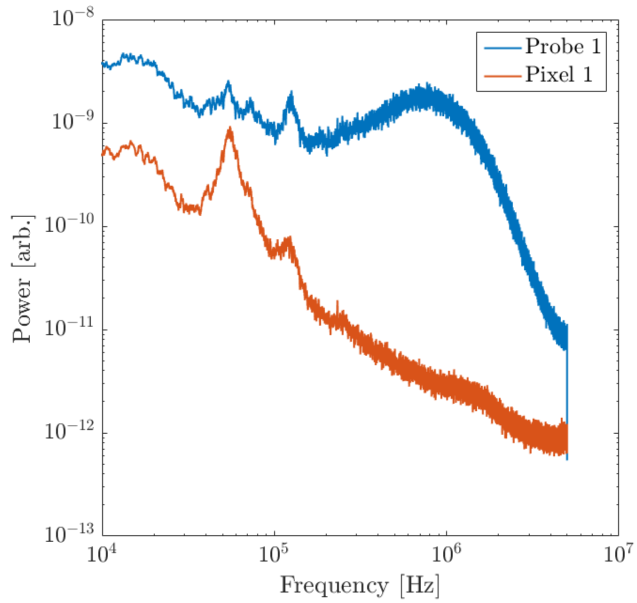

Figure 6: A comparison of the frequency content from probe 1 and pixel 1 on the SiPM at 55 A and 5 sccm. This shows a difference in the high frequency response.

Using the analysis technique presented in Sec. C, the dispersion of the plasma was estimated using the probe and SiPM measurements. A comparison of the dispersion is shown in Fig. 7. Fig. 7a shows an acoustic relationship between the wavevector and frequency, or $\omega \propto k$, for the probes. Fig. 7b shows that the dispersion estimated with the SiPM array is also acoustic in nature. The dispersion is well above the noise in the probe measurements while the SiPM is just above the noise.

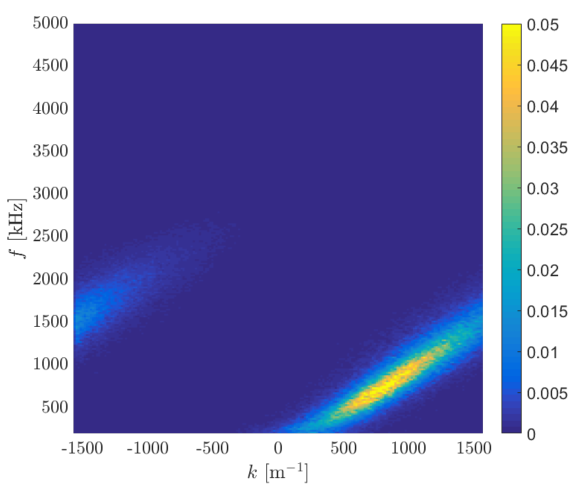

(a) Dispersion estimated using the probes for the H6 hollow cathode at 55 A and 5 sccm.

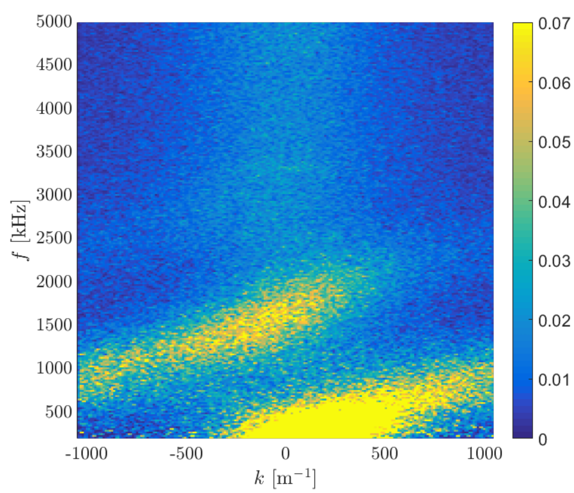

(b) Dispersion estimated using the SiPM for the H6 hollow cathode at 55 A and 5 sccm.

Figure 7: Comparison of the dispersion of the probes and SiPM.

The weaker response by the SiPM technique could be a combination of multiple effects. The SiPM measurement is radially line integrated through the cathode plume. Because the acoustic waves are turbulent, the phase at any point in the plasma may be different than the phase at the object plane. Spatially integrating over all these components should cause the signal to get averaged out, reducing the signal to noise. An additional consideration is that the assumptions made in the analysis in Sec. B may be overly simplified and that fluctuations in light intensity are not strictly proportional to fluctuations in plasma density. Lastly, the detector is also limited by the photon rate. If the frequency of the wave is larger than the rate at which photons can be generated as a result of the change in plasma density, then the light intensity may not be proportional to the plasma density. All of these effects may be contributing to the low signal to noise in the dispersion estimated by the SiPM measurements. Although additional work is required to identify more precisely how these deleterious effects limit the signal, the experimental configuration was modified to collect light from a 3×3 mm^2 area in the plasma to investigate how the signal is affected by the collection area of the SiPM. The measurement in this configuration could not resolve the IAT, probably because the frequency cutoff (from Eqn. 18) at around 1 MHz. From this result, we conclude that spatial averaging can certainly play a role in the signal to noise.

The last point of comparison between the SiPM and the probes is phase velocity measurement. The data in Fig. 7 is phase wrapped because of k_{max} associated with the configuration of the probes and SiPM. This means that the negative values of k in Fig. 7 are actually aliased values of k that are larger than k_{max}. This phase wrapping can be corrected for by concatenating our initial result with a shifted (in k) data set. The results of this analysis are shown in Fig. 8. Fig. 8a shows the unwrapped dispersion for the probes and Fig. 8b shows the corrected SiPM dispersion at 55 A and 5 sccm. The phase velocity was determined by curve fitting the unwrapped data. with Eqn. 19.

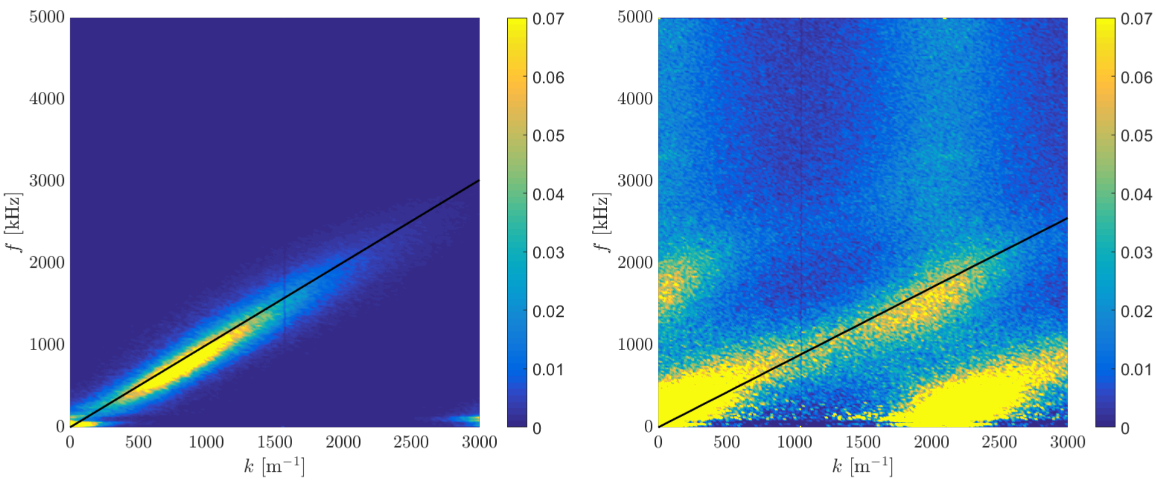

(a) unwrapped data for the probes at the 55 A and 5 sccm operating condition. The best fit line shows a phase velocity of 5.3 ± 1.4 km/s.

(b) unwrapped data for the probes at the 55 A and 5 sccm operating condition. The best fit line shows a phase velocity of 4.8 ± 1.6 km/s.

Figure 8: Comparison of the phase wrapping corrected data between the probes and SiPM.

The phase velocity measured at a few current conditions is shown in Fig 9. The uncertainty in the phase velocity is derived from the width of the probe (SiPM). Below 50 A, the IAT spectrum was not measurable with the SiPM due to the signal to noise ratio at high frequency, however, the measurements that were observable above 50 A show a similar trend to the probe measurements. Both the probes and SiPM are within uncertainty of the data collected by Jorns of a 100-A hollow cathode at 8 sccm.[8]

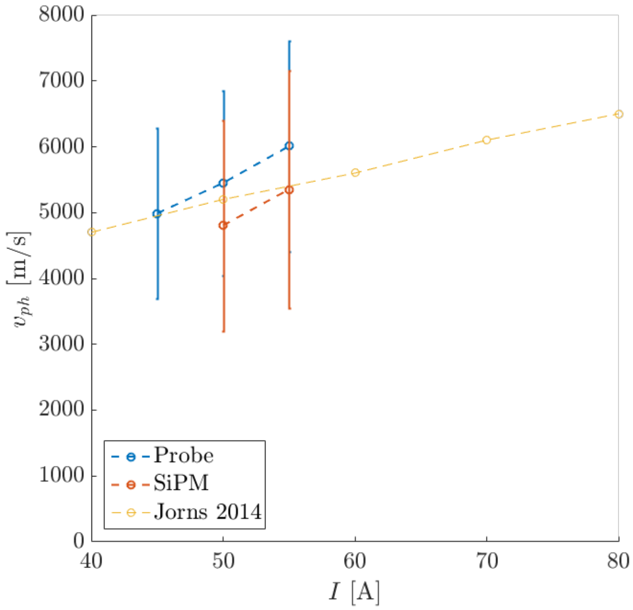

Figure 9: The measured phase velocity as a function of current at a mass flow rate of 5 sccm. The reference data is in good agreement on a 100 A hollow cathode is in agreement with the measurements on the H6 cathode. Probe data is in blue, SiPM in red and reference data is in yellow.[8] The reference data was acquired on a 100-A hollow cathode at 8 sccm.

V. Conclusions

An approach for non-invasively estimating the dispersion in an electric propulsion plasma has been developed using an SiPM as a optical measurement device. Fluctuations in the light emitted from the plasma are shown to be proportional to the fluctuation in plasma density under the assumption of isothermality and small neutral density fluctuations. The dispersion measured with the SiPM technique is shown to be within uncertainty of the probe measurements. Futhermore, the phase velocity is shown to agree with reference data published by Jorns et al.[8] The SiPM technique is advantageous over the probe technique in that it does not perturb the plasma, but the signal to noise suffers due to the phase averaging over line the integration and the is restricted by the image size on the SiPM pixels.

Future work on this diagnostic will reduce the image size on the pixels to eliminate the problems with frequency bandwidth. In addition, this new diagnostic can be used to implement a planar laser induced fluorescence (LIF) scheme to measure the spatial evolution of the ion velocity distribution. Further development may include a planar time-resolved LIF scheme that can resolve the Hall thruster breathing mode. Lastly this diagnostic may permit the non-invasive estimation of dispersion in the near-field of a Hall thruster, which may provide clues to the electron cross field transport problem in Hall thruster numerical codes.

VI. Acknowledgments

This work was funded by NASA Space Technology Research Fellowship grant NNX15AQ37H. The authors also would like to thank the electric propulsion group at NASA GRC for providing the anode for this experiment.

References

[1] Brophy, J., Garner, C., Nakazono, B., Marcucci, M., Henry, M., and Noon, D., "The Ion Propulsion System for Dawn," American Institute of Aeronautics and Astronautics, July 2003.

[2] Hruby, V., Spence, D., Demmons, N., Roy, T., Ehrbar, E., Zwahlen, J., Martin, R., Ziemer, J., Connolly,

W., Rhodes, S., and Tolman, W., "ST7-DRS Colloid Thruster System Development and Performance Summary," American Institute of Aeronautics and Astronautics, July 2008.

3 MarreeseReading, C., "Microfluidic Electrospray Propulsion(MEP) Thruster Performance with Microfabricated Emitter Arrays for Indium Propellant," American Institute of Aeronautics and Astronautics, July 2016.

4 McDonald, M. A., Caram, J. M., Lopez, P., Hinkel, H. D., Bowie, J. T., Abell, P. A., Drake, B. G., Martinez, R. M., Chodas, P. W., Hack, K., and others, "Extensibility of human asteroid mission to Mars and other destinations," *Space Ops 13th International Conference on Space Operations*, 2014.

5 Hofer, R. R., Herman, D., Polk, J. E., Kamhawi, H., and Mikellides, I. G., "Development Approach and Status of the 12.5 kW HERMeS Hall Thruster for the Solar Electric Propulsion Technology Demonstration Mission," *34th International Electric Propulsion Conference, Hyogo-Kobe, Japan, IEPC-2015-186*, 2015.

6 Mikellides, I. G., Katz, I., Goebel, D. M., and Jameson, K. K., "Evidence of nonclassical plasma transport in hollow cathodes for electric propulsion," *Journal of Applied Physics*, Vol. 101, No. 6, March 2007, pp. 063301.

7 Jorns, B., Lopez Ortega, A., and Mikellides, I. G., "First-principles Modelling of the IAT-driven Anomalous Resistivity in Hollow Cathode Discharges I: Theory," American Institute of Aeronautics and Astronautics, July 2016.

8 Jorns, B. A., Mikellides, I. G., and Goebel, D. M., "Ion acoustic turbulence in a 100-A LaB6 hollow cathode," *Physical Review E*, Vol. 90, No. 6, Dec. 2014, pp. 063106.

9 Yanes, N., Jorns, B., Friss, A., Polk, J. E., Guerrero, P., and Austin, J. M., "Ion Acoustic Turbulence and Ion Energy Measurements in the Plume of the HERMeS Thruster Hollow Cathode," American Institute of Aeronautics and Astronautics, July 2016.

10 Jorns, B., Goebel, D. M., and Hofer, R. R., "Plasma Perturbations in High-Speed Probing of Hall Thruster Discharge Chambers: Quantification and Mitigation," American Institute of Aeronautics and Astronautics, July 2015.

11 Grimaud, L., Ptin, A., Vaudolon, J., and Mazouffre, S., "Perturbations induced by electrostatic probe in the discharge of Hall thrusters," *Review of Scientific Instruments*, Vol. 87, No. 4, April 2016, pp. 043506.

12 Beall, J. M., Kim, Y. C., and Powers, E. J., "Estimation of wavenumber and frequency spectra using fixed probe pairs," *Journal of Applied Physics*, Vol. 53, No. 6, June 1982, pp. 3933–3940.

13 Kanik, I., Johnson, P. V., and James, G. K., "Electron-impact-induced emission and excitation cross sections of xenon at low energies," *Journal of Physics B: Atomic, Molecular and Optical Physics*, Vol. 34, No. 9, 2001, pp. 1685.